JACS
JOURNAL OF THE AMERICAN CHEMICAL SOCIETY

pubs.acs.org/JACS

Article

Unraveling the Excited-State Dynamics and Light-Harvesting Functions of Xanthophylls in Light-Harvesting Complex II Using Femtosecond Stimulated Raman Spectroscopy

Juan M. Artes Vivancos,* Ivo H. M. van Stokkum, Francesco Saccon, Yusaku Hontani, Miroslav Kloz, Alexander Ruban, Rienk van Grondelle, and John T. M. Kennis*

Cite This: J. Am. Chem. Soc. 2020, 142, 17346−17355

Read Online

ACCESS | Metrics & More | Article Recommendations | Supporting Information

ABSTRACT: Photosynthesis in plants starts with the capture of photons by light-harvesting complexes (LHCs). Structural biology and spectroscopy approaches have led to a map of the architecture and energy transfer pathways between LHC pigments. Still, controversies remain regarding the role of specific carotenoids in light-harvesting and photoprotection, obligating the need for high-resolution techniques capable of identifying excited-state signatures and molecular identities of the various pigments in photosynthetic systems. Here we demonstrate the successful application of femtosecond stimulated Raman spectroscopy (FSRS) to a multichromophoric biological complex, trimers of LHCII. We demonstrate the application of global and target analysis (GTA) to FSRS data and utilize it to quantify excitation migration in LHCII trimers. This powerful combination of techniques allows us to obtain valuable insights into structural, electronic, and dynamic information from the carotenoids of LHCII trimers. We report spectral and dynamical information on ground- and excited-state vibrational modes of the different pigments, resolving the vibrational relaxation of the carotenoids and the pathways of energy transfer to chlorophylls. The lifetimes and spectral characteristics obtained for the S1 state confirm that lutein 2 has a distorted conformation in LHCII and that the lutein 2 S1 state does not transfer to chlorophylls, while lutein 1 is the only carotenoid whose S1 state plays a significant energy-harvesting role. No appreciable energy transfer takes place from lutein 1 to lutein 2, contradicting recent proposals regarding the functions of the various carotenoids (Son et al. *Chem.* **2019**, 5 (3), 575−584). Also, our results demonstrate that FSRS can be used in combination with GTA to simultaneously study the electronic and vibrational landscapes in LHCs and pave the way for in-depth studies of photoprotective conformations in photosynthetic systems.

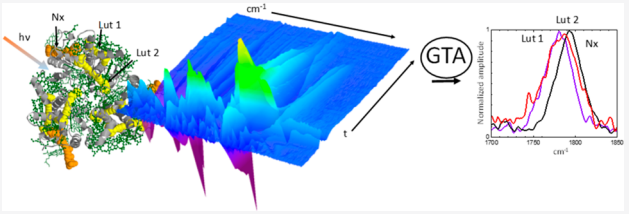

INTRODUCTION

Photosynthesis is the biological process that harvests solar energy, sustaining most life on earth.[1,2] A complete understanding of the mechanisms involved and the factors that modulate photosystem efficiency constitutes an interdisciplinary challenge that could provide the basis for the design of the next generation of sustainable and highly efficient light-conversion devices,[3−6] a pressing need in todays global changing climate.[7]

In the photosynthetic apparatus, membrane-associated pigment−protein complexes organize in photosystems that harvest energy and transfer it toward a reaction center.[1,2] Light-harvesting complex II (LHCII) is the most abundant protein in plant thylakoid membranes. It organizes into trimers and serves different functions: under moderate light, it harvests excitation energy, while in high-light conditions, it switches to a dissipative state to protect the system from photodamage.[2,8]

Recent structural biology studies provided a complete picture of the structural organization of this complex in plants (Figure 1A−C).[9−11] Figure 1 shows the LHCII structure with its pigments: 14 chlorophylls (Chls) and 4 carotenoids (Cars) per monomer. Chls absorb light in the red (600−700 nm) and blue (400−500 nm) and constitute clusters optimized to delocalize the excitation, providing efficient transfer pathways.[12−14] Cars play fundamental roles in maintaining the integrity of the protein and protect the complex from harmful Chl triplet states.[15,16] They also participate in light-harvesting, with blue-green (around 500 nm) light stimulating the transition to the second excited state (S2), which then can transfer energy to Chls.[17] The first excited (S1) state of Cars is of particular interest: it is a dark state that has the same A_g^- symmetry as the ground state and therefore symmetry-forbidden for optical transitions from the ground state. Given its adjustable energetic alignment with Chl excited

Received: April 27, 2020
Published: September 3, 2020

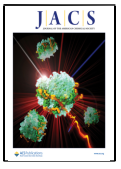

https://dx.doi.org/10.1021/jacs.0c04619
J. Am. Chem. Soc. 2020, 142, 17346−17355

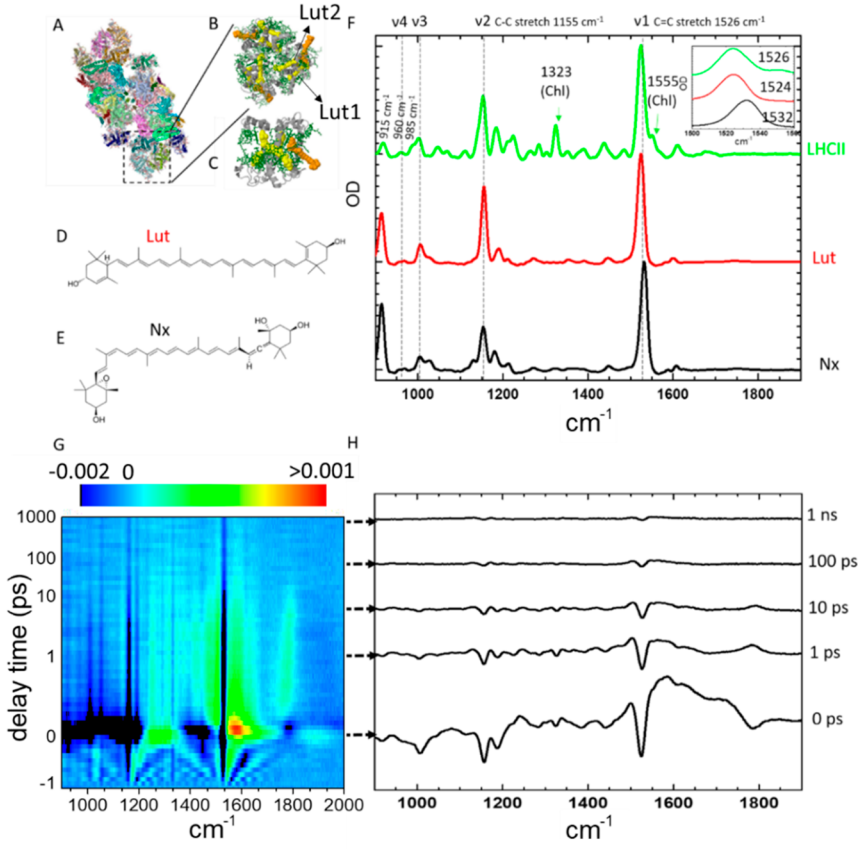

Figure 1. (A) The molecular structure of the LHCII-PSII supercomplex from spinach[32] (PDB ID: 3JCU), an LHCII trimer is indicated with a square. (B) The molecular structure of the LHCII trimer from a top view and (C) an LHCII monomer viewed from the side. (D) The molecular structure of the xanthophyll lutein (yellow in B, C). (E) The molecular structure of the xanthophyll neoxanthin (orange in B, C). (F) Ground-state stimulated Raman spectra for LHCII trimers in buffer−detergent solution at pH 7.6 (green trace), lutein in THF (red), and neoxanthin in THF (black). The inset shows a close-up of the C═C stretch region. (G) Heat map for a typical FSRS experiment on LHCII (495 nm excitation). Blue colors correspond to a negative signal, while bright green corresponds to positive signals. Note that the nonzero signals at short negative delay times close to zero correspond to coherent artifacts resulting from the three-pulse interaction. (H) Selected transient Raman spectra from G, at times indicated by the dashed arrows.

states, the Car S1 state has been proposed and experimentally observed to participate both in light-harvesting[18−22] and in de-excitation processes.[6,23−27] In oxygenic photosynthesis, its involvement is an essential determinant of light-harvesting efficiency, and it has been suggested to be involved in the regulation of having LHCs in the light-harvesting or energy dissipating state.[18,19,22,28−31]

Figure 1D,E shows the chemical structures of the two principal Cars in LHCII trimer preparations: lutein (Lut) and neoxanthin (Nx). LHCII trimers in native membranes bind some other carotenoids,[32,33] but these are present only in trace amounts in purified LHCII trimer preparations in detergent−buffer solutions (see Table S1 and Figure S1 in SI).[26] Lut and Nx are xanthophylls that play diverse roles in LHCII with distinct molecular structures. Nx is tightly bound to LHCII,[34] in a peripheral pocket near a Chl *b* cluster,[35] and it is in the cis conformation.[36] Luteins are found in two separate pockets and are spectrally distinct[37] and referred to as Lut1 and Lut2. Lut1 (maximum absorption ∼495 nm, lutein 1620 in ref 32) is essential for the structural integrity of LHCII,[35] and Lut2 (maximum absorption ∼510 nm, lutein 1621[32]) is required for trimerization.[38] All these different properties result in specific spectroscopic signatures. Energy transfer dynamics in LHCII trimers involving Chl and Cars have been studied using a variety of time-resolved experimental[18,19,21,24,39−41] and computational[42,43] techniques. Also, vibrational spectroscopy led to structural insights into the carotenoids bound to LHCII and their plasticity in response to changes in LHCII light-harvesting function.[24,44] However, the detailed xanthophyll excited-state dynamics of LHCII are still unclear, as it is difficult to distinguish their spectral signatures with typically used techniques such as ultrafast transient absorption spectroscopy (TAS). For this reason, the light-harvesting and photoprotection roles of the specific xanthophylls presently remain controversial.[18,19,24,39−41] In a recent 2DES study it was proposed that extensive energy transfer would take place from Lut1 to Lut2, and that therefore Lut2 would constitute the nexus of the xanthophyll light-harvesting function in LHCII trimers.[41]

There is a clear need for testing and validating the models behind the involvement of xanthophylls' excited states in light-harvesting and photoprotective photosynthetic processes. Disentanglement of the xanthophyll excited-state dynamics is therefore essential. A technique that combines ultrafast time-resolved and vibrational approaches, femtosecond stimulated Raman spectroscopy (FSRS),[45−49] could fill this gap. FSRS yields superior resolution relative to traditional TAS experiments, providing both detailed structural and electronic information in complex biomolecules. On the other hand, FSRS is challenging because it requires separating the Raman

https://dx.doi.org/10.1021/jacs.0c04619
J. Am. Chem. Soc. 2020, 142, 17346−17355

signal from coherent nonresonant signals, and unwanted pump−probe and pump-dump/repump−probe signals, which result in significant uncertainties regarding baselines. To overcome these limitations, we have recently developed a variation of the technique based on spectral watermarking that allows recovery of the fs-Raman response with high fidelity.[50−53]

Herein we investigate the dynamics of the vibrational modes of the pigments involved in the light-harvesting phase of photosynthesis in plants. By selective excitation in the carotenoid region, this technique provides high-resolution insights into the dynamics of the pigment excited states. With this novel application of FSRS to a complex photosynthetic system, we obtain structural and electronic information. Using global and target analysis (GTA)[54] on FSRS data, we resolve spectral signatures and lifetimes for each pigment, including vibrational relaxation and their contribution to the LHCII energy-harvesting function. These results show that the only S1 state contributing to light-harvesting is that of Lut1, while S1 states from the other xanthophylls may fulfill different roles in photosynthesis. In contrast to the findings of a recent report,[41] our results exclude that any appreciable energy transfer occurs from Lut1 to Lut2, contradicting that the latter would constitute the nexus of the carotenoid light-harvesting function in LHCII.

RESULTS AND DISCUSSION

Figure 1F shows the stimulated Raman spectrum with a preresonant Raman pump at 800 nm for the ground state (GS) of LHCII (green), indicating the main vibrational modes typical for carotenoid molecules.[55,56] Vibrations around 1530 cm^{-1} correspond to the C═C stretching in the conjugated chain (ν1). This mode is often used as a fingerprint of the identity of the carotenoid in resonance Raman experiments[55,56] because its frequency is dependent on the conjugation length of the molecule. In Figure 1F, we obtain 1526 cm^{-1}, in agreement with resonance Raman experiments on LHCII in the literature.[55,56]

To confirm the identity of the spectral signatures in the LHCII−protein samples, we also performed experiments on the carotenoids contained in our LHCII samples (Lut and Nx) in tetrahydrofuran (THF). Figure 1F shows the GS stimulated Raman for LHCII trimers (in green) compared to the ones obtained for Lut (red) and Nx (black) in THF. The GS signal from LHCII trimers is an intricate convolution of multiple contributions, but the ν1 frequency is closer to that obtained for Lut in THF (1526 cm^{-1} for LHCII trimers vs. 1524 and 1532 cm^{-1} for Lut and Nx in the THF solution, respectively, cf. the inset of Figure 1F), consistent with the pigment composition (2:1 ratio Lut:Nx, see Table S1). Some bands are only present in the LHCII trimers while absent in THF (at 1329 and 1555 cm^{-1}, indicated with green arrows in Figure 1F) and correspond to Chl. In particular, the peak found at 1555 cm^{-1} corresponds to Chl ring breathing.[57,58]

Figure 1G shows the fs-ns FSRS of LHCII trimers by exciting Car with a 495 nm actinic pump. These spectra result from subtracting the GS Raman from the excited-state signal for each delay time after processing through the watermarking process.[50] In Figure 1H, we show selected FSRS spectra at different delay times from Figure 1G. While there are positive signals, the most prominent features are negative signals that contain information about the ground-state bleach (GSB) of different vibrational modes of the LHCII trimers. While artifacts can obscure the quantitative interpretation of GSB in FSRS,[59] these negative signals contain information about the pigments excited, mainly Cars. We may thus interpret the excited carotenoid dynamics correlating the peak positions with the extensive literature of resonance Raman.[8,33,37,55,56] These FSRS results also show positive features that reveal the excited-state dynamics of carotenoids. Around 200 fs, a new positive feature appears at about 1750 cm^{-1} (see Figure 1G), shifts to 1780 cm^{-1} after around 1 ps, and decays while shifting to higher frequencies. This signal is positive because it appears in the excited-state Raman, while it is absent in the GS. The peak position corresponds to an unusually upshifted value for the C═C stretching frequency in the optically forbidden S1 state of carotenoids, which results from the strong vibronic coupling between the S0 and S1 states.[60] Such bands have been observed before with picosecond resonant Raman and FSRS experiments in the S1 state of carotenoids in solution,[50,61−63] in a cyanobacterial light-harvesting complex,[52] and a UV-absorbing rhodopsin.[53] These features are analyzed with GTA, interpreted, and discussed in more detail below. We also performed FSRS experiments on LHCII with actinic pump excitation at 520 and 486 nm, targeting different LHCII pigment populations.

A sequential scheme could well describe FSRS experiments performed on Lut and Nx in THF with four components, cf. Figure S5A,B. Figure 2 shows the species associated difference spectra (SADS) estimated by GTA. This experiment allows for resolving the S2−S1−S0 excited-state relaxation and vibrational relaxation in the S1 state. The magenta SADS correspond to S2, the blue and cyan SADS correspond to successive hot S1, partially relaxed S1, and the red or black SADS correspond to fully relaxed S1. The development of the S1 band occurs near 1790 cm^{-1}. The S2 state shows a broad positive signal at the high-frequency side of the C═C stretch, similar to that reported previously for β-carotene,[62] although we did not observe a broad absorption in the 1000−1400 cm^{-1} region as in ref 62 (note that the convention for representing FSRS spectra differs between this work and refs 61 and 62 in this work; difference spectra featuring GSB are presented, whereas, in the latter, FSRS spectra were corrected for ground-state bands). The S2 state decays with 0.23 and 0.31 ps in Lut and Nx, respectively, consistent with previous reports on xanthophylls.[19,20]

Concomitant with the decay of the S2 state, the vibrationally excited S1 state is formed, signified by the appearance of a positive C═C stretch band at 1763 cm^{-1} for Lut and Nx. (blue lines). The first stage of vibrational relaxation occurs with time constants of 0.46 or 0.53 ps, consistent with earlier reports on β-carotene,[61,64] and involves a rise and an upshift of the S1 C═C band from 1763 to 1783 cm^{-1} for Lut and from 1763 to 1780 cm^{-1} for Nx. We resolve a second, previously unknown phase in the vibrational relaxation process of the S1 state of 1.1 ps, which corresponds to a further upshift of the S1 C═C band to 1795 and 1790 cm^{-1}, for Lut and Nx, respectively.

Note that the SADS representing the S1 states show a broad negative baseline in the region between 1600 and 1800 cm^{-1}. This is a consequence of the watermarking approach, which causes broad negative features to appear on either side of positive bands (the "sombrero shape" effect), and should be interpreted as an incomplete baseline removal rather than genuine negative signals, as we described previously.[50,53] Furthermore, we note that in the S1 state, there is still

https://dx.doi.org/10.1021/jacs.0c04619
J. Am. Chem. Soc. 2020, 142, 17346−17355

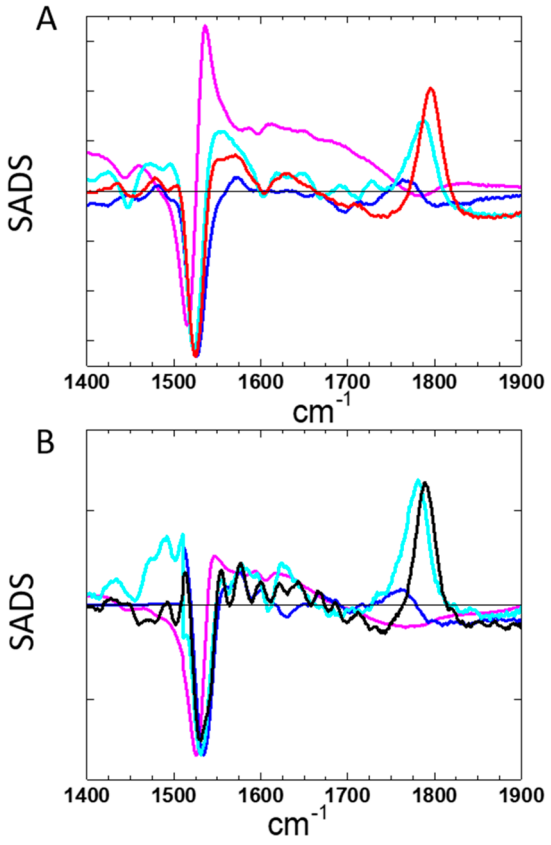

Figure 2. SADS estimated from sequential analysis using a kinetic scheme S2 → first hot S1 → second hot S1 → relaxed S1 of FSRS experiments performed on (A) lutein and (B) neoxanthin in THF. Key: (A) 0.23 (magenta), 0.46 (blue), 1.1 (cyan) and 11 ps (red) and (B) 0.31 (magenta), 0.53 (blue), 1.1 (cyan) and 39 ps (black). The magenta and blue SADS have been scaled for comparison (see Figure S2 for unscaled full spectra).

intensity of the C═C stretch mode around 1525 cm^{-1}, i.e., the intensity does not entirely shift toward ~1790 cm^{-1}, as shown for β-carotene with picosecond Raman spectroscopy.[63] There the C═C band slightly upshifted and broadened in the S1 state as compared to the S0 ground state. In the S1 spectra of Lut and Nx, where we present the S1 minus S0 FSRS spectrum, this may give rise to the positive-going signals around the GSB near 1525 cm^{-1}.

The fully relaxed S1 state decays with 11 and 39 ps in Lut and Nx, respectively, in agreement with the literature.[20,65] Lut has a shorter S1 lifetime, as expected for a longer conjugation length of the polyene backbone.[20] The C═C frequency of the relaxed S1 state of Nx is slightly lower (1790 cm^{-1}) as compared to that of Lut (1795 cm^{-1}). These lifetimes and spectral characteristics are necessary to interpret the SADS obtained from the GTA on LHCII below.

First, we present the results from global analysis (GA) for the FSRS data taken on LHCII trimers excited at 520 nm (Figure S5D), at the very red edge of the LHCII xanthophyll absorption (Figure S1). Under these conditions, Lut2 is selectively excited,[66] with no significant contributions from Lut1, Nx, or Chl, which allows us to record its FSRS signature and its contribution to the spectral evolution. This GA describes the data with the help of independent exponential decays and their amplitudes, the decay-associated difference spectra (DADS). In this global analysis, three lifetimes are estimated: 0.46 ps, 20 ps, and 1.7 ns. Because of the limited signal-to-noise (due to the relatively low pumping efficiency at 520 nm), we could not resolve the S2 and hot S1 states and hence are represented by an average lifetime and an average DADS. The black DADS represents the decay of the Lut2 S2 and hot S1 (peaking around 1560 cm^{-1} with a shoulder around 1740 cm^{-1}) in 0.46 ps, as well as the rise of the Lut2 S1 (negative amplitudes from 1790 to 1810 cm^{-1}). The red DADS represents the decay of the Lut2 S1 (peaking around 1790 cm^{-1}) in 20 ps. Finally, the green DADS represents the decay of Chl in 1.7 ns.

Figure 3A shows the kinetic scheme used to analyze the FSRS data upon 520 nm excitation using GTA. As mentioned

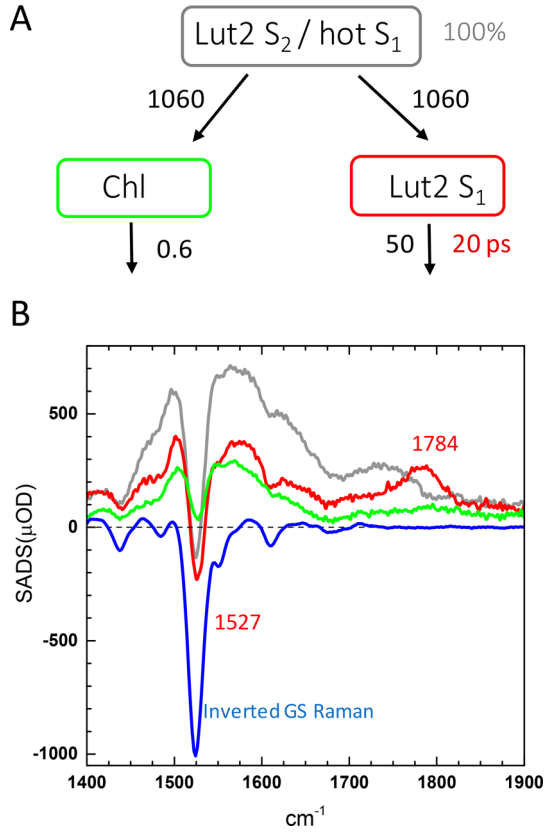

Figure 3. Target analysis of the fs-Raman data of LHCII trimers after 520 nm excitation. A. The kinetic model of energy transfer in LHCII, consisting of three compartments, all rate constants are in ns^{-1}. B. SADS key: Lut2 S2/hot S1 (gray), Lut2 S1 (red), and Chl (green). Inverted GS Raman of LHCII trimers (blue) for comparison.

above, we could not resolve the S2 and hot S1 states, which are now taken together in a single compartment (gray). The actinic pump thus excites Lut2 to the S2 state that is assumed to branch (in 0.5 ps) equally to Chl (green compartment) and the S1 state (red compartment). We note that when a compartment branches (the gray one in this case), only the total decay rate can be directly estimated. Thus, one has to make an assumption on the branching fractions, which affects only the relative populations, and therefore only the relative amplitudes of the Chl and S1 SADS.

The Lut2 S2/hot S1 SADS (Figure 3B, gray line) shows a broad upshift of the ν1 band, as observed for Lut in solution (Figure 2), along with the signature of the hot S1 state near 1750 cm^{-1}. Besides, it shows GSB around 1527 cm^{-1},

https://dx.doi.org/10.1021/jacs.0c04619
J. Am. Chem. Soc. 2020, 142, 17346−17355

consistent with the specific excitation of Lut.[66] A peak of around 1784 cm^{-1} characterizes the Lut2 S1 SADS (red line). Its lifetime is 20 ps, which is unusually long for a carotenoid with 10 conjugated double bonds.[20] The implications of these observations will be discussed further below. The Chl SADS (green line) has a low amplitude and a lifetime of a few nanoseconds. It shows a negative dip of the carotenoid C═C stretch frequency, consistent with the observations in the cyanobacterial light-harvesting protein HliC, where it was assigned to an inner filter effect due to excited-state absorption of Chl at 800 nm, which partly absorbs the Raman pump. This causes a spurious bleach of all Raman bands,[52] of which the carotenoid C═C stretches are dominant.

With 486 and 495 nm excitation, a mixture of pigments is excited, i.e., Lut, Nx, and Chl. First, we employ a global analysis, which has only a minimal number of assumptions. Both 486 and 495 nm excitation will share common lifetimes because they will only differ in the relative excitation patterns of Lut, Nx, and Chl. Therefore, we performed a global analysis of the two data sets and estimated five common lifetimes of 125 fs, 0.53 ps, 4.4 ps, 34 ps, and 2.4 ns. The estimated DADS are collated in Figure 4. They can be interpreted as follows.

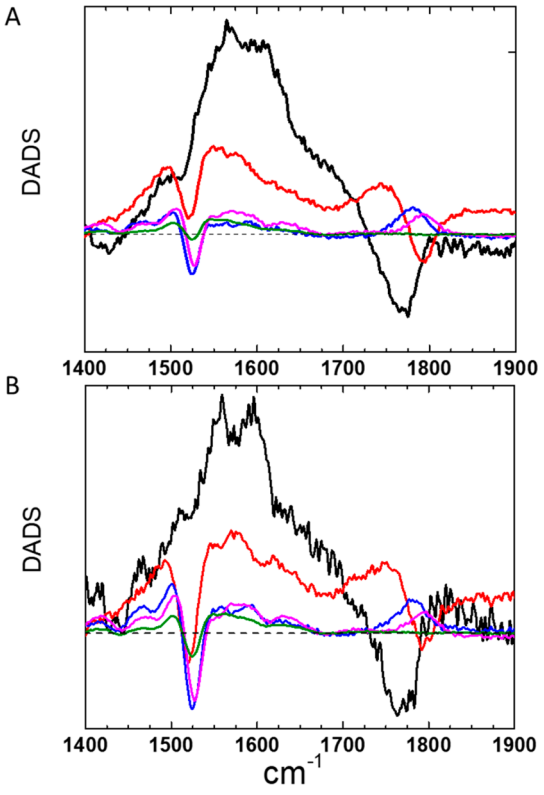

Figure 4. DADS estimated from a global analysis of the (A) 495 and (B) 486 nm excitation experiments. Key: 125 fs (black), 0.53 ps (red), 4.4 ps (blue), 34 ps (magenta), and 2.4 ns (green).

The black DADS represent the decay of the Lut and Nx S2 (peaking around 1600 cm^{-1}) in 125 fs, as well as the rise of the Lut and Nx hot S1 (negative amplitudes from 1740 to 1790 cm^{-1}). The red DADS represent the decay of the Lut and Nx hot S1 (peaking around 1750 cm^{-1}) in 0.53 ps, as well as the rise of the Lut and Nx S1 (negative amplitudes around 1790 cm^{-1}). Both the black and red lines are mixtures of Lut and Nx states represented by an average lifetime and an average DADS. The blue DADS represent the decay of an S1 state that peaks at 1781 cm^{-1} in 4.4 ps. The magenta DADS represent the decay of an S1 state that peaks at 1793 cm^{-1} in 34 ps. Finally, the green DADS represent the decay of Chl in 2.4 ns. The state that peaks at 1781 cm^{-1} can be assigned to Lut S1, and the relatively short lifetime (4.4 ps) compared to the solution (11 ps) can be attributed to excitation energy transfer (EET) from Lut S1 to Chl. The state that peaks at 1793 cm^{-1} can be assigned to Nx S1, and because its lifetime (34 ps) is almost the same as in THF solution (39 ps), there is practically no EET to Chl. We note that the amplitude of the S2 DADS is significantly larger than that of the S1 state: this is due to the more favorable resonance of the S2 excited-state absorption with the 800 nm Raman pump as compared to that of the S1 state.

These observations have led us to propose the kinetic scheme of Figure 5A for GTA of the FSRS data sets. The

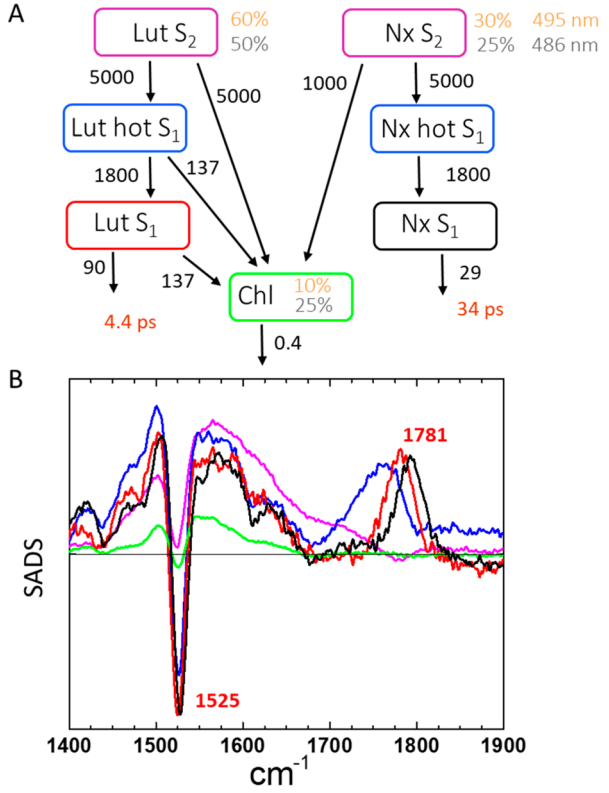

Figure 5. (A) Kinetic scheme for the GTA of the 495 and 486 nm excitation experiments, with input fractions in orange and gray, respectively. All rate constants are in ns^{-1}. (B) SADS estimated with 495 nm excitation. Key: Lut1 and Nx S2 (magenta), Lut1 and Nx hot S1 (blue), Lut1 S1 (red), Nx S1 (black), and Chl (green). The magenta and blue SADS have been scaled for comparison (see Figure S4 for the full spectra).

model considers the direct excitation of Lut, Nx, and Chl with the fractions indicated in the figure (see methods in SI) and follows the photophysics of carotenoids in addition to energy transfer processes. Lut and Nx are excited to their S2 states. From the Nx and Lut S2 states, there is a competition between energy transfer to Chl and internal conversion to their respective hot S1 states. The hot S1 state vibrationally cools to the relaxed S1 state but may also show energy transfer to Chl. In the Lut relaxed S1 state, there is a competition between energy transfer to Chl and internal conversion to the ground

https://dx.doi.org/10.1021/jacs.0c04619
J. Am. Chem. Soc. 2020, 142, 17346−17355

state. As there is no energy transfer from the Nx S1 state to Chl, it only decays by internal conversion to the ground state.

In the target analysis, we did not make any distinction between Chl *a* and Chl *b* because the Chl FSRS signature is dominated by carotenoid features, as observed previously for HliC.[52] This model constitutes a minimal representation of the energy transfer pathways and is consistent with those proposed previously.[18,19,21] The figure also shows the rates (in ns^{-1}) by which the compartments evolve. Lut and Nx are excited to the S2 state, for which the same SADS is assumed (magenta in Figure 5). Lut S2 transfers energy to Chl in competition with internal conversion to the (hot) S1 state. For Lut, the S2 lifetime is fixed at 100 fs, and branching to Chl and hot S1 (set at 1:1), in agreement with earlier studies.[18,19,21] The energy transfer from the Nx S2 state to Chl was set to 1000 ns^{-1}.[21] The vibrational cooling processes of the S1 state upon relaxation from S2 cannot be distinguished between Lut and Nx; thus, we again assume the same SADS (blue in Figure 5). This model formalizes the features of the excited-state evolution that became apparent in the GA of Figure 4.

In contrast to Lut and Nx in solution (see Figure 2), we resolve only a single phase in the vibrational cooling process. From the Lut S1 state, energy transfer to Chl occurs in competition with internal conversion to the ground state. The rate constant for the latter is fixed at 90 ns^{-1}, the value that we found for Lut in solution (Figure 2, 11 ps lifetime). The sum of the estimated rate constant for energy transfer, 137 ns^{-1}, and that of internal conversion, 90 ns^{-1}, yields a Lut S1 lifetime of 4.4 ps. The Nx S1 state has the same lifetime as in THF solution (Figure 2), which implies that it internally converts to the ground state without transferring energy to Chl in this model (see the lifetime discussion below). The transfer ratios to Chl obtained in these analyses is in the same range of previously reported experimental studies.[21]

Figure 5B shows the SADS estimated from the GTA with 495 nm excitation. Figure S5 demonstrates that 486 and 495 nm excitation SADS agree. The S2 and hot S1 SADS (magenta and blue) are consistent with those of Lut and Nx in solution (Figure 2), with a broad upshifted C═C band from 1530 to 1650 cm^{-1} for S2 and an upshifted C═C band for the hot S1 state around 1760 cm^{-1}. Strikingly, the relaxed S1 SADS of Lut and Nx (red and black) are well resolved, with the S1 band peaking at 1781 cm^{-1} for Lut and at 1793 cm^{-1} for Nx. The lifetime for the Lut S1 state of 4.4 ps is smaller than the 11 ps found in THF, indicating that the Lut S1 state efficiently transfers energy to Chl. In contrast, the lifetime estimated for the Nx S1 is 34 ps (internal conversion rate is constant 29 ns^{-1}), only slightly lower than in THF, indicating virtually no light-harvesting role for the Nx S1 state. Finally, the green SADS corresponds to Chl, with a lifetime in the nanosecond range.[16,18,67] We could not detect an appreciable population of Lut2 upon 486 and 495 nm excitation.

Overseeing the FSRS results with the three excitation wavelengths 486, 495, and 520 nm, we have identified the spectral signature and lifetime of the optically forbidden S1 state of the three distinct xanthophylls. Figure 6 shows a comparison of their SADS, which are different in spectral signature and lifetime. With 520 nm, Lut2 is selectively populated, showing an S1 band at 1784 cm^{-1}, which has a 20 ps lifetime (red line). With 486 and 495 nm excitation, we identify a Lut S1 band around 1781 cm^{-1}, which has a 4.4 ps lifetime (violet line), and an Nx band at 1791 cm^{-1} with a 34 ps lifetime (black line). Given that the 1784 cm^{-1} band

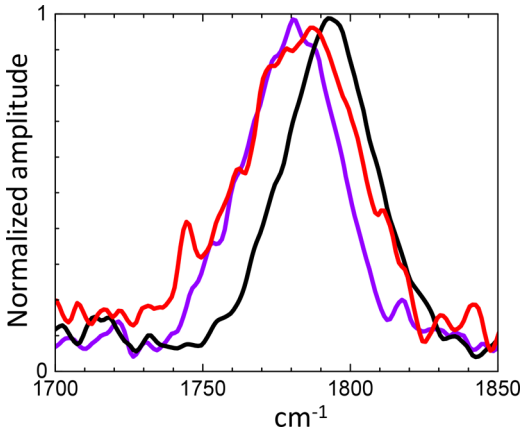

Figure 6. Detail of the S1 C═C Raman bands for the different xanthophylls in LHCII; Lut1 (violet, from the data at 495 nm excitation), Lut2 (red, from the data at 520 nm excitation), and Nx (black, from the data at 486 nm excitation). The SADS were normalized, remaining baseline corrected and smoothed for clarity.

belongs to Lut2, we conclude that the 1781 cm^{-1} that is populated upon 486 and 495 nm must belong mainly to Lut1. From our results, we obtained information on the pathways and rates of energy transfer to Chl. Lut1 and Lut2 both transfer energy to Chl from the S2 state on a 100 fs time scale. Lut1 is the only xanthophyll where the S1 state transfers energy to Chl on the picosecond time scale; for Nx and Lut2, this can be excluded, given their S1 lifetimes of 34 and 20 ps.

In solution, Lut shows a higher frequency in the relaxed S1 state than Nx (1795 and 1790 cm^{-1}, respectively, Figure 2), whereas in LHCII trimers, Nx shows the highest frequency (1793 cm^{-1}) while Lut1 and Lut2 are found at 1781 and 1784 cm^{-1}, respectively. These opposite trends require clarification. In carotenoids, the S1 C═C frequency is determined by the S1 energy level and the extent of vibronic coupling between S1 and S0 states (and to a lesser extent, the vibronic coupling between S2 and S1 states).[68] The vibronic couplings depend on the molecular symmetry: with perfect C_{2h} symmetry, the coupling is maximal, while for less symmetric systems, the coupling is smaller. A higher S1 energy level leads to a higher S1 frequency due to a decreased π electron delocalization; likewise, a larger vibronic coupling will lead to a higher S1 frequency. In THF solution, the S1 energy level of Nx is higher than that of Lut, but at the same time, Nx is less symmetric than Lut. The net effect of these counteracting effects on the S1 frequency may be a lower S1 frequency in Nx as compared to Lut, which is experimentally observed.

We observe that in LHCII, the S1 frequency of Nx is very similar to that in THF (1793 and 1790 cm^{-1}, respectively), whereas the S1 frequencies of Lut1 and Lut2 are significantly downshifted in LHCII with respect to THF (1781 and 1784 cm^{-1} versus 1795 cm^{-1}). We interpret this effect as arising from the tuning of the lutein S1 properties in the LHCII binding pocket, in particular the S1 energy levels.[69] This is consistent with the idea that the properties of Lut have been significantly affected in LHCII and those of Nx to a lesser extent. Also, the vibronic coupling in Lut1 and Lut2 may have been affected by structural distortions of the polyene backbone and their ε and β rings, with ensuing slight departures from C_{2h} symmetry, which may result in S1 frequency downshifts.

Lut2 exhibits rather remarkable properties. Its S2 absorption is red-shifted with respect to that of Lut1, but it shows a higher

https://dx.doi.org/10.1021/jacs.0c04619
J. Am. Chem. Soc. 2020, 142, 17346−17355

S1 frequency than Lut1 (1784 vs 1781 cm^{-1}), and an unusually long S1 lifetime of 20 ps, much longer than Lut in solution (11 ps, Figure 2 and previous results[20]). These observations suggest higher S1 energy for Lut2 as compared to Lut1. This is likely related to a distortion of its conjugated π-electron system,[37] resulting in a reduced effective conjugation length, an elevated S1 energy level, and a longer S1 lifetime. Such a situation would be extraordinary because the Lut2 S2 energy is lower in Lut2 as compared to Lut1. Thus, even though the Lut2 backbone is distorted and the effective conjugation length diminished, effectively elevating S1, its S2 energy is stabilized, presumably through dipolar interactions in the binding pocket that are specific to trimerization. We note that the unique properties of Lut2 in LHCII trimers are absent in LHCII monomers: in the latter system, Lut2 is spectroscopically indistinguishable from Lut1.[16,21]

It is interesting to compare the situation of Lut1 and Lut2 in LHCII trimers with that for β-carotene in HliC.[52] HliC is an ancestral LH protein of cyanobacteria, where the β-carotene S1 state efficiently quenches the Chl *a* excited state in picoseconds.[70] Two β-carotenes were identified in HliC; β-car1 and β-car2, where β-car1 accepts energy from Chl and exhibits a low S1 C=C frequency of 1774 cm^{-1}, and β-car2 does not receive energy from Chl,[52] with β-car2 showing a high S1 C=C frequency of 1780 cm^{-1}. These findings, common to different photosynthetic organisms (relatively distant in evolutionary terms), suggest that some fundamental architecture and mechanism involving specialization and electronic tuning of carotenoids have been selected to maximize efficiency while enabling photoprotection, integrating these mechanisms in the natural photosynthetic molecular design.

Our FSRS results on LHCII trimers are in agreement with the concept of the protein pocket tuning Car electronic structure via optimizing the geometry.[41,52,71] However, they are also at odds with the picture recently proposed based on 2DES spectroscopy by Son et al.[41] In that paper, Lut2 is proposed as the nexus of xanthophyll energy transfer to Chl; Lut1 would donate energy from its S2 state to the Lut2 S2 state, which in turn would transfer energy to Chl. This scenario is incompatible with our findings because we observe the Lut1 S1 state upon 486 and 495 nm excitation, which would not, or hardly, be populated if the Lut1 S2 state would transfer to Lut2 before internal conversion to the S1 state. Also, if that were the case, we would observe the Lut2 S1 state upon Lut1 excitation, because energy transfer from Lut2 to Chl occurs in competition with internal conversion to S1. We can exclude such a scenario based on the observed S1 frequency and lifetime after Lut1 excitation. In the same recent paper,[41] an unidentified Sx state was proposed, which had a lifetime of 300 fs and was involved in energy transfer. We note that the Lut1 hot S1 state has a similar lifetime of 500 fs. Hence, the proposed Sx state could well correspond to the Lut1 hot S1 state. Further combined experimental and theoretical studies are needed to map the excited states in photosynthetic antenna unambiguously. However, our results show that the only carotenoid transferring efficiently to Chl from the S1 state is Lut1, while Nx and Lut2 may have been optimized for different roles.[38,72,73]

We have shown here that the properties of Cars have been finely tuned by the protein matrix to enable distinct light-harvesting functions, primarily for Lut1 and Lut2. Here Lut1 has an efficient light-harvesting role, which, given its distinctly low S1 C=C frequency, likely results from a lowered S1 energy level and/or a reduced C_{2h} symmetry, which may favor energetic matching and an optimized electronic coupling with Chl. Lut2 does not exhibit an efficient light-harvesting function from its S1 state. Instead, we observe an unusually long S1 lifetime of 20 ps and a higher S1 C=C stretch than Lut1, which is likely due to an elevated S1 energy level that may result from a decreased effective conjugation length. We note that Lut2 plays an essential role in the quenching of Chl triplet states,[16] which may come at the expense of its light-harvesting efficiency.

The question arises how such properties may be modified to enable the switch into a photoprotective mode, which is activated in the thylakoid membrane under excess light conditions.[2,8,74] Various lines of evidence point at subtle conformational changes in LHCII under such quenching conditions that involve Chls and Cars.[24,75−78] In particular, Nx obtains a twisted conformation under quenching conditions,[24] and Lut1 was proposed to act as a quencher of Chl excited states, through direct energy transfer,[24,79] excitonic interactions[78] or charge transfer.[80] The protein and pigments change conformation in a way that we do not entirely understand yet, but lutein likely undergoes geometrical changes and distortions that change energetics and electronic couplings with Chl.[76,77] We have shown here, by assessing the vibrational signatures of the S1 states in LHCII, that such tuning applies to the two luteins in the light-harvesting conformation, which lends credibility to the idea that their conformational plasticity underlies the switching capacity to the dissipative state of LHCII. The FSRS technique may provide the key to assess these long-standing issues in future quantitative studies.

CONCLUSION

In summary, we applied FSRS to LHCII and obtained signatures of the vibrational modes for the different pigments. Our results confirm that energy transfer from the carotenoid S2 states to chlorophylls occurs on a subpicosecond time scale and that only the S1 state of Lut1 transfers energy to the chlorophyll population. These findings pave the way to more detailed studies on the vibrational signatures of excited states and their role in photosynthesis mechanisms and regulation.

EXPERIMENTAL DETAILS

Femtosecond Stimulated Raman Spectroscopy (FSRS). Femtosecond stimulated Raman experiments were performed with the watermarking nearly baseline-free stimulated Raman setup reported previously.[50−52] Briefly, the Raman pump (800 nm, ∼7 μJ) and the Raman probe (∼840−960 nm) were spatiotemporally overlapped at the sample position. The actinic pump (520 nm, 495 or 486 nm, ∼280 nJ) was focused on the sample. The probe light was dispersed by a spectrograph (Acton SpectraPro SP-2500, Princeton Instruments) and detected by a 1024-pixel back-thinned FFT-CCD detector (S7030−1007, Hamamatsu). A narrow-band ($\Delta \sim 10$ nm) interference filter was used for each excitation wavelength. Seventy time points were measured from −500 fs to 1.5 ns. The instrument response function of this setup is in the 85−160 fs range.[53] Spectra for Figure 6 were corrected for remaining minor baselines[50] by subtracting a constant value, normalized, and smoothed for clarity by adjacent averaging with a five-point window using Origin Pro 8.

ASSOCIATED CONTENT

Supporting Information

The Supporting Information is available free of charge at https://pubs.acs.org/doi/10.1021/jacs.0c04619.

https://dx.doi.org/10.1021/jacs.0c04619
J. Am. Chem. Soc. 2020, 142, 17346−17355

Additional experimental methods, Table S1, Figures S1−S6, and additional references (PDF)

AUTHOR INFORMATION

Corresponding Authors

Juan M. Artes Vivancos − *Department of Physics and Astronomy and LaserLaB, Faculty of Science, Vrije Universiteit Amsterdam, 1081 HV Amsterdam, The Netherlands; Department of Chemistry, Kennedy College of Science, University of Massachusetts—Lowell, Lowell, Massachusetts 01854, United States;* orcid.org/0000-0002-5050-3760; Email: juan_artesvivancos@uml.edu

John T. M. Kennis − *Department of Physics and Astronomy and LaserLaB, Faculty of Science, Vrije Universiteit Amsterdam, 1081 HV Amsterdam, The Netherlands;* orcid.org/0000-0002-3563-2353; Email: j.t.m.kennis@vu.nl

Authors

Ivo H. M. van Stokkum − *Department of Physics and Astronomy and LaserLaB, Faculty of Science, Vrije Universiteit Amsterdam, 1081 HV Amsterdam, The Netherlands;* orcid.org/0000-0002-6143-2021

Francesco Saccon − *Queen Mary University of London, School of Biological and Chemical Sciences, E1 4NS London, U.K.*

Yusaku Hontani − *Department of Physics and Astronomy and LaserLaB, Faculty of Science, Vrije Universiteit Amsterdam, 1081 HV Amsterdam, The Netherlands;* orcid.org/0000-0001-8853-9454

Miroslav Kloz − *Department of Physics and Astronomy and LaserLaB, Faculty of Science, Vrije Universiteit Amsterdam, 1081 HV Amsterdam, The Netherlands*

Alexander Ruban − *Queen Mary University of London, School of Biological and Chemical Sciences, E1 4NS London, U.K.*

Rienk van Grondelle − *Department of Physics and Astronomy and LaserLaB, Faculty of Science, Vrije Universiteit Amsterdam, 1081 HV Amsterdam, The Netherlands*

Complete contact information is available at: https://pubs.acs.org/10.1021/jacs.0c04619

Notes

The authors declare no competing financial interest.

ACKNOWLEDGMENTS

This project has received funding from the European Union's Horizon2020 program under the Marie Skłodowska-Curie grant agreements no. 660521 to J.M.A.V. and no. 675006 to FS. The NWO supported Y.H. and J.T.M.K. through a VICI grant, and a Middelgroot investment grant to J.T.M.K. A.V.R. acknowledges the support from the Royal Society Wolfson Research Merit Award WRMA2015/R1. M.K. was supported by Grant Agency of the Czech Republic project number 17-01137S. RvG was supported by an Advanced Investigator Grant from the European Research Council (no. 267333, PHOTPROT), the TOP-grant (700.58.305) from the Foundation of Chemical Science part of NWO, and the Canadian Institute for Advanced Research (CIFAR). R.v.G. gratefully acknowledges his Academy Professor grant from The Netherlands Royal Academy of Sciences (KNAW).

ABBREVIATIONS

LHCs, light-harvesting complexes; LHCII, light-harvesting complex II; FSRS, femtosecond-stimulated Raman spectroscopy; GA, global analysis; GS, ground state; GTA, global and target analysis; Chl, chlorophyll; Car, carotenoid; Lut, lutein; Nx, neoxanthin; TAS, transient absorption spectroscopy; GSB, ground-state bleach; SADS, species-associated decay spectrum; DADS, decay-associated difference spectra

REFERENCES

(1) Blankenship, R. E. *Molecular mechanisms of photosynthesis*; John Wiley & Sons: Hoboken, NJ, 2014.

(2) Croce, R.; Van Grondelle, R.; Van Amerongen, H.; Van Stokkum, I. *Light Harvesting in Photosynthesis*; CRC Press: Boca Raton, 2018.

(3) Scholes, G. D.; Fleming, G. R.; Olaya-Castro, A.; Van Grondelle, R. Lessons from nature about solar light harvesting. *Nat. Chem.* **2011**, *3* (10), 763.

(4) Odella, E.; Mora, S. J.; Wadsworth, B. L.; Huynh, M. T.; Goings, J. J.; Liddell, P. A.; Groy, T. L.; Gervaldo, M.; Sereno, L. E.; Gust, D.; Moore, T. A.; Moore, G. F.; Hammes-Schiffer, S.; Moore, A. L. Controlling Proton-Coupled Electron Transfer in Bioinspired Artificial Photosynthetic Relays. *J. Am. Chem. Soc.* **2018**, *140* (45), 15450−15460.

(5) Sokol, K. P.; Robinson, W. E.; Oliveira, A. R.; Warnan, J.; Nowaczyk, M. M.; Ruff, A.; Pereira, I. A. C.; Reisner, E. Photoreduction of CO_2 with a Formate Dehydrogenase Driven by Photosystem II Using a Semi-artificial Z-Scheme Architecture. *J. Am. Chem. Soc.* **2018**, *140* (48), 16418−16422.

(6) Kloz, M.; Pillai, S.; Kodis, G.; Gust, D.; Moore, T. A.; Moore, A. L.; van Grondelle, R.; Kennis, J. T. M. Carotenoid Photoprotection in Artificial Photosynthetic Antennas. *J. Am. Chem. Soc.* **2011**, *133* (18), 7007−7015.

(7) Lenton, T. M.; Latour, B. Gaia 2.0. *Science* **2018**, *361* (6407), 1066.

(8) Ruban, A. V.; Johnson, M. P.; Duffy, C. D. The photoprotective molecular switch in the photosystem II antenna. *Biochim. Biophys. Acta, Bioenerg.* **2012**, *1817* (1), 167−181.

(9) Su, X.; Ma, J.; Wei, X.; Cao, P.; Zhu, D.; Chang, W.; Liu, Z.; Zhang, X.; Li, M. Structure and assembly mechanism of plant C2S2M2-type PSII-LHCII supercomplex. *Science* **2017**, *357* (6353), 815−820.

(10) Liu, Z.; Yan, H.; Wang, K.; Kuang, T.; Zhang, J.; Gui, L.; An, X.; Chang, W. Crystal structure of spinach major light-harvesting complex at 2.72 Å resolution. *Nature* **2004**, *428* (6980), 287.

(11) Standfuss, J.; van Scheltinga, A. C. T.; Lamborghini, M.; Kühlbrandt, W. Mechanisms of photoprotection and nonphotochemical quenching in pea light-harvesting complex at 2.5 Å resolution. *EMBO J.* **2005**, *24* (5), 919−928.

(12) Novoderezhkin, V. I.; Palacios, M. A.; Van Amerongen, H.; Van Grondelle, R. Excitation dynamics in the LHCII complex of higher plants: modeling based on the 2.72 Å crystal structure. *J. Phys. Chem. B* **2005**, *109* (20), 10493−10504.

(13) Connelly, J.; Müller, M.; Hucke, M.; Gatzen, G.; Mullineaux, C.; Ruban, A.; Horton, P.; Holzwarth, A. Ultrafast spectroscopy of trimeric light-harvesting complex II from higher plants. *J. Phys. Chem. B* **1997**, *101* (10), 1902−1909.

(14) Zhang, Z.; Lambrev, P. H.; Wells, K. L.; Garab, G.; Tan, H.-S. Direct observation of multistep energy transfer in LHCII with fifth-order 3D electronic spectroscopy. *Nat. Commun.* **2015**, *6*, 7914.

(15) Peterman, E.; Dukker, F. M.; Van Grondelle, R.; Van Amerongen, H. Chlorophyll a and carotenoid triplet states in light-harvesting complex II of higher plants. *Biophys. J.* **1995**, *69* (6), 2670−2678.

(16) Gall, A.; Berera, R.; Alexandre, M. T.; Pascal, A. A.; Bordes, L.; Mendes-Pinto, M. M.; Andrianambinintsoa, S.; Stoitchkova, K. V.; Marin, A.; Valkunas, L.; et al. Molecular adaptation of photoprotection: triplet states in light-harvesting proteins. *Biophys. J.* **2011**, *101* (4), 934−942.

(17) Ruban, A. V. Identification of carotenoids in photosynthetic proteins: Xanthophylls of the light harvesting antenna. In *Carotenoids*

Physical, Chemical, and Biological Functions and Properties; Landrum, J. T., Ed.; CRC Press: Boca Raton, 2010; pp 113−136.
(18) Gradinaru, C. C.; van Stokkum, I. H. M.; Pascal, A. A.; van Grondelle, R.; van Amerongen, H. Identifying the pathways of energy transfer between carotenoids and chlorophylls in LHCII and CP29. A multicolor, femtosecond pump− probe study. *J. Phys. Chem. B* **2000**, *104* (39), 9330−9342.
(19) Holt, N. E.; Kennis, J.; Dall'Osto, L.; Bassi, R.; Fleming, G. R. Carotenoid to chlorophyll energy transfer in light harvesting complex II from Arabidopsis thaliana probed by femtosecond fluorescence upconversion. *Chem. Phys. Lett.* **2003**, *379* (3−4), 305−313.
(20) Polívka, T.; Sundström, V. Ultrafast dynamics of carotenoid excited states− from solution to natural and artificial systems. *Chem. Rev.* **2004**, *104* (4), 2021−2072.
(21) Croce, R.; Muller, M. G.; Bassi, R.; Holzwarth, A. R. Carotenoid-to-Chlorophyll Energy Transfer in Recombinant Major Light-Harvesting Complex (LHCII) of Higher Plants. I. Femtosecond Transient Absorption Measurements. *Biophys. J.* **2001**, *80* (2), 901−915.
(22) Polivka, T.; Frank, H. A. Molecular Factors Controlling Photosynthetic Light Harvesting by Carotenoids. *Acc. Chem. Res.* **2010**, *43* (8), 1125−1134.
(23) Berera, R.; Herrero, C.; Van Stokkum, I. H.; Vengris, M.; Kodis, G.; Palacios, R. E.; Van Amerongen, H.; Van Grondelle, R.; Gust, D.; Moore, T. A.; et al. A simple artificial light-harvesting dyad as a model for excess energy dissipation in oxygenic photosynthesis. *Proc. Natl. Acad. Sci. U. S. A.* **2006**, *103* (14), 5343−5348.
(24) Ruban, A. V.; Berera, R.; Ilioaia, C.; Van Stokkum, I. H.; Kennis, J. T.; Pascal, A. A.; Van Amerongen, H.; Robert, B.; Horton, P.; Van Grondelle, R. Identification of a mechanism of photoprotective energy dissipation in higher plants. *Nature* **2007**, *450* (7169), 575−578.
(25) Liguori, N.; Xu, P.; van Stokkum, I. H.; van Oort, B.; Lu, Y.; Karcher, D.; Bock, R.; Croce, R. Different carotenoid conformations have distinct functions in light-harvesting regulation in plants. *Nat. Commun.* **2017**, *8* (1), 1994.
(26) Mascoli, V.; Liguori, N.; Xu, P.; Roy, L. M.; van Stokkum, I. H. M.; Croce, R. Capturing the Quenching Mechanism of Light-Harvesting Complexes of Plants by Zooming in on the Ensemble. *Chem.* **2019**, *5* (11), 2900−2912.
(27) Staleva, H.; Komenda, J.; Shukla, M. K.; Slouf, V.; Kana, R.; Polivka, T.; Sobotka, R. Mechanism of photoprotection in the cyanobacterial ancestor of plant antenna proteins. *Nat. Chem. Biol.* **2015**, *11* (4), 287−U96.
(28) Holt, N. E.; Kennis, J. T. M.; Fleming, G. R. Femtosecond fluorescence upconversion studies of light harvesting by β-carotene in oxygenic photosynthetic core proteins. *J. Phys. Chem. B* **2004**, *108* (49), 19029−19035.
(29) de Weerd, F. L.; Kennis, J. T. M.; Dekker, J. P.; van Grondelle, R. β-Carotene to chlorophyll singlet energy transfer in the photosystem I core of Synechococcus elongatus proceeds via the β-carotene S-2 and S-1 states. *J. Phys. Chem. B* **2003**, *107* (24), 5995−6002.
(30) de Weerd, F. L.; Dekker, J. P.; van Grondelle, R. Dynamics of β-carotene-to-chlorophyll singlet energy transfer in the core of photosystem II. *J. Phys. Chem. B* **2003**, *107* (25), 6214−6220.
(31) Kennis, J. T. M.; Gobets, B.; van Stokkum, I. H. M.; Dekker, J. P.; van Grondelle, R.; Fleming, G. R. Light harvesting by chlorophylls and carotenoids in the photosystem I core complex of *Synechococcus elongatus*: A fluorescence upconversion study. *J. Phys. Chem. B* **2001**, *105* (19), 4485−4494.
(32) Wei, X.; Su, X.; Cao, P.; Liu, X.; Chang, W.; Li, M.; Zhang, X.; Liu, Z. Structure of spinach photosystem II−LHCII supercomplex at 3.2 Å resolution. *Nature* **2016**, *534* (7605), 69.
(33) Ruban, A. V. *The photosynthetic membrane: molecular mechanisms and biophysics of light harvesting*; John Wiley & Sons: Hoboken, NJ, 2013.
(34) Ruban, A. V.; Lee, P. J.; Wentworth, M.; Young, A. J.; Horton, P. Determination of the stoichiometry and strength of binding of xanthophylls to the photosystem II light harvesting complexes. *J. Biol. Chem.* **1999**, *274* (15), 10458−10465.
(35) Croce, R.; Weiss, S.; Bassi, R. Carotenoid-binding sites of the major light-harvesting complex II of higher plants. *J. Biol. Chem.* **1999**, *274* (42), 29613−29623.
(36) Ruban, A. V.; Pascal, A. A.; Robert, B.; Horton, P. Configuration and Dynamics of Xanthophylls in Light-Harvesting Antennae of Higher Plants. Spectroscopic Analysis of Isolated Light-Harvesting Complex of Photosystem II and Thylakoid Membranes. *J. Biol. Chem.* **2001**, *276* (27), 24862−24870.
(37) Ruban, A. V.; Pascal, A. A.; Robert, B. Xanthophylls of the major photosynthetic light-harvesting complex of plants: identification, conformation and dynamics. *FEBS Lett.* **2000**, *477* (3), 181−185.
(38) Dall' Osto, L.; Lico, C.; Alric, J.; Giuliano, G.; Havaux, M.; Bassi, R. Lutein is needed for efficient chlorophyll triplet quenching in the major LHCII antenna complex of higher plants and effective photoprotection in vivo under strong light. *BMC Plant Biol.* **2006**, *6* (1), 32.
(39) van Oort, B.; van Grondelle, R.; van Stokkum, I. H. A hidden state in light-harvesting complex II revealed by multipulse spectroscopy. *J. Phys. Chem. B* **2015**, *119* (16), 5184−5193.
(40) Van Oort, B.; Roy, L. M.; Xu, P.; Lu, Y.; Karcher, D.; Bock, R.; Croce, R. Revisiting the role of xanthophylls in nonphotochemical quenching. *J. Phys. Chem. Lett.* **2018**, *9* (2), 346−352.
(41) Son, M.; Pinnola, A.; Bassi, R.; Schlau-Cohen, G. S. The electronic structure of lutein 2 is optimized for light harvesting in plants. *Chem.* **2019**, *5* (3), 575−584.
(42) Duffy, C.; Chmeliov, J.; Macernis, M.; Sulskus, J.; Valkunas, L.; Ruban, A. Modeling of fluorescence quenching by Lutein in the plant light-harvesting complex LHCII. *J. Phys. Chem. B* **2013**, *117* (38), 10974−10986.
(43) Duffy, C.; Valkunas, L.; Ruban, A. Quantum mechanical calculations of xanthophyll−chlorophyll electronic coupling in the light-harvesting antenna of photosystem II of higher plants. *J. Phys. Chem. B* **2013**, *117* (25), 7605−7614.
(44) Robert, B.; Horton, P.; Pascal, A. A.; Ruban, A. V. Insights into the molecular dynamics of plant light-harvesting proteins in vivo. *Trends Plant Sci.* **2004**, *9* (8), 385−390.
(45) Kukura, P.; McCamant, D. W.; Mathies, R. A. Femtosecond stimulated Raman spectroscopy. *Annu. Rev. Phys. Chem.* **2007**, *58*, 461−488.
(46) Shim, S.; Dasgupta, J.; Mathies, R. A. Femtosecond Time-Resolved Stimulated Raman Reveals the Birth of Bacteriorhodopsin's J and K Intermediates. *J. Am. Chem. Soc.* **2009**, *131* (22), 7592−7597.
(47) Fang, C.; Frontiera, R. R.; Tran, R.; Mathies, R. A. Mapping GFP structure evolution during proton transfer with femtosecond Raman spectroscopy. *Nature* **2009**, *462* (7270), 200.
(48) Oscar, B. G.; Liu, W.; Zhao, Y.; Tang, L.; Wang, Y.; Campbell, R. E.; Fang, C. Excited-state structural dynamics of a dual-emission calmodulin-green fluorescent protein sensor for calcium ion imaging. *Proc. Natl. Acad. Sci. U. S. A.* **2014**, *111* (28), 10191−10196.
(49) Kukura, P.; McCamant, D. W.; Yoon, S.; Wandschneider, D. B.; Mathies, R. A. Structural observation of the primary isomerization in vision with femtosecond-stimulated Raman. *Science* **2005**, *310* (5750), 1006−1009.
(50) Kloz, M.; Weißenborn, J.; Polívka, T.; Frank, H. A.; Kennis, J. T. Spectral watermarking in femtosecond stimulated Raman spectroscopy: resolving the nature of the carotenoid S* state. *Phys. Chem. Chem. Phys.* **2016**, *18* (21), 14619−14628.
(51) Hontani, Y.; Inoue, K.; Kloz, M.; Kato, Y.; Kandori, H.; Kennis, J. T. The photochemistry of sodium ion pump rhodopsin observed by watermarked femto-to submillisecond stimulated Raman spectroscopy. *Phys. Chem. Chem. Phys.* **2016**, *18* (35), 24729−24736.
(52) Hontani, Y.; Kloz, M.; Polivka, T.; Shukla, M.; Sobotka, R.; Kennis, J. T. Molecular Origin of Photoprotection in Cyanobacteria Probed by Watermarked Femtosecond Stimulated Raman Spectroscopy. *J. Phys. Chem. Lett.* **2018**, *9* (7), 1788−1792.

https://dx.doi.org/10.1021/jacs.0c04619
J. Am. Chem. Soc. 2020, 142, 17346−17355

(53) Hontani, Y.; Broser, M.; Luck, M.; Weissenborn, J.; Kloz, M.; Hegemann, P.; Kennis, J. T. M. Dual Photoisomerization on Distinct Potential Energy Surfaces in a UV-Absorbing Rhodopsin. *J. Am. Chem. Soc.* **2020**, *142* (26), 11464−11473.
(54) van Stokkum, I. H. M.; Larsen, D. S.; van Grondelle, R. Global and target analysis of time-resolved spectra. *Biochim. Biophys. Acta, Bioenerg.* **2004**, *1657* (2), 82−104.
(55) Robert, B. Resonance Raman spectroscopy. *Photosynth. Res.* **2009**, *101* (2−3), 147−155.
(56) Ruban, A. V.; Horton, P.; Robert, B. Resonance Raman spectroscopy of the photosystem II light-harvesting complex of green plants: a comparison of trimeric and aggregated states. *Biochemistry* **1995**, *34* (7), 2333−2337.
(57) Lutz, M. Resonance Raman spectra of chlorophyll in solution. *J. Raman Spectrosc.* **1974**, *2* (5), 497−516.
(58) Lutz, M. Antenna chlorophyll in photosynthetic membranes. A study by resonance Raman spectroscopy. *Biochim. Biophys. Acta, Bioenerg.* **1977**, *460* (3), 408−430.
(59) Kloz, M.; van Grondelle, R.; Kennis, J. T. M. Correction for the time dependent inner filter effect caused by transient absorption in femtosecond stimulated Raman experiment. *Chem. Phys. Lett.* **2012**, *544*, 94−101.
(60) Nagae, H.; Kuki, M.; Zhang, J. P.; Sashima, T.; Mukai, Y.; Koyama, Y. Vibronic coupling through the in-phase, C═C stretching mode plays a major role in the 2A(g)(−) to 1A(g)(−) internal conversion of *all-trans-β*-carotene. *J. Phys. Chem. A* **2000**, *104* (18), 4155−4166.
(61) McCamant, D. W.; Kukura, P.; Mathies, R. A. Femtosecond time-resolved stimulated Raman spectroscopy: application to the ultrafast internal conversion in *β*-carotene. *J. Phys. Chem. A* **2003**, *107* (40), 8208−8214.
(62) Kukura, P.; McCamant, D. W.; Mathies, R. A. Femtosecond time-resolved stimulated Raman spectroscopy of the S2 ($1Bu^+$) excited state of *β*-carotene. *J. Phys. Chem. A* **2004**, *108* (28), 5921.
(63) Hashimoto, H.; Koyama, Y.; Hirata, Y.; Mataga, N. S1 and T1 species of. beta.-carotene generated by direct photoexcitation from the all-trans, 9-cis, 13-cis, and 15-cis isomers as revealed by picosecond transient absorption and transient Raman spectroscopies. *J. Phys. Chem.* **1991**, *95* (8), 3072−3076.
(64) De Weerd, F. L.; Van Stokkum, I. H.; Van Grondelle, R. Subpicosecond dynamics in the excited state absorption of all-trans-*β*-carotene. *Chem. Phys. Lett.* **2002**, *354* (1−2), 38−43.
(65) Polívka, T.; Sundström, V. Dark excited states of carotenoids: consensus and controversy. *Chem. Phys. Lett.* **2009**, *477* (1−3), 1−11.
(66) Mendes-Pinto, M. M.; Galzerano, D.; Telfer, A.; Pascal, A. A.; Robert, B.; Ilioaia, C. Mechanisms underlying carotenoid absorption in oxygenic photosynthetic proteins. *J. Biol. Chem.* **2013**, *288* (26), 18758−18765.
(67) Pandit, A.; Shirzad-Wasei, N.; Wlodarczyk, L. M.; van Roon, H.; Boekema, E. J.; Dekker, J. P.; de Grip, W. J. Assembly of the major light-harvesting complex II in lipid nanodiscs. *Biophys. J.* **2011**, *101* (10), 2507−2515.
(68) Noguchi, T.; Hayashi, H.; Tasumi, M.; Atkinson, G. H. Solvent Effects on the A_g C═C Stretching Mode in the 2^1A_g-Excited-State of Beta-Carotene and 2 Derivatives - Picosecond Time-Resolved Resonance Raman-Spectroscopy. *J. Phys. Chem.* **1991**, *95* (8), 3167−3172.
(69) Polivka, T.; Zigmantas, D.; Sundstrom, V.; Formaggio, E.; Cinque, G.; Bassi, R. Carotenoid S-1 state in a recombinant light-harvesting complex of photosystem II. *Biochemistry* **2002**, *41* (2), 439−450.
(70) Staleva, H.; Komenda, J.; Shukla, M. K.; Šlouf, V.; Kaňa, R.; Polívka, T.; Sobotka, R. Mechanism of photoprotection in the cyanobacterial ancestor of plant antenna proteins. *Nat. Chem. Biol.* **2015**, *11* (4), 287.
(71) Llansola-Portoles, M. J.; Sobotka, R.; Kish, E.; Shukla, M. K.; Pascal, A. A.; Polívka, T.; Robert, B. Twisting a *β*-carotene, an adaptive trick from nature for dissipating energy during photoprotection. *J. Biol. Chem.* **2017**, *292* (4), 1396−1403.
(72) Mozzo, M.; Dall' Osto, L.; Hienerwadel, R.; Bassi, R.; Croce, R. Photoprotection in the antenna complexes of photosystem II - Role of individual xanthophylls in chlorophyll triplet quenching. *J. Biol. Chem.* **2008**, *283* (10), 6184−6192.
(73) Pascal, A. A.; Liu, Z. F.; Broess, K.; van Oort, B.; van Amerongen, H.; Wang, C.; Horton, P.; Robert, B.; Chang, W. R.; Ruban, A. Molecular basis of photoprotection and control of photosynthetic light-harvesting. *Nature* **2005**, *436* (7047), 134−137.
(74) Croce, R.; van Amerongen, H. Natural strategies for photosynthetic light harvesting. *Nat. Chem. Biol.* **2014**, *10* (7), 492−501.
(75) Pandit, A.; Reus, M.; Morosinotto, T.; Bassi, R.; Holzwarth, A. R.; de Groot, H. J. M. An NMR comparison of the light-harvesting complex II (LHCII) in active and photoprotective states reveals subtle changes in the chlorophyll a ground-state electronic structures. *Biochim. Biophys. Acta, Bioenerg.* **2013**, *1827* (6), 738−744.
(76) Balevicius, V.; Fox, K. F.; Bricker, W. P.; Jurinovich, S.; Prandi, I. G.; Mennucci, B.; Duffy, C. D. P. Fine control of chlorophyll-carotenoid interactions defines the functionality of light-harvesting proteins in plants. *Sci. Rep.* **2017**, *7*, 10.
(77) Fox, K. F.; Balevicius, V.; Chmeliov, J.; Valkunas, L.; Ruban, A. V.; Duffy, C. D. P. The carotenoid pathway: what is important for excitation quenching in plant antenna complexes? *Phys. Chem. Chem. Phys.* **2017**, *19* (34), 22957−22968.
(78) Ilioaia, C.; Johnson, M. P.; Liao, P. N.; Pascal, A. A.; van Grondelle, R.; Walla, P. J.; Ruban, A. V.; Robert, B. Photoprotection in Plants Involves a Change in Lutein 1 Binding Domain in the Major Light-harvesting Complex of Photosystem II. *J. Biol. Chem.* **2011**, *286* (31), 27247−27254.
(79) Berera, R.; van Grondelle, R.; Kennis, J. T. M. Ultrafast transient absorption spectroscopy: principles and application to photosynthetic systems. *Photosynth. Res.* **2009**, *101* (2−3), 105−118.
(80) Cupellini, L.; Calvani, D.; Jacquemin, D.; Mennucci, B. Charge transfer from the carotenoid can quench chlorophyll excitation in antenna complexes of plants. *Nat. Commun.* **2020**, *11* (1), 8.

https://dx.doi.org/10.1021/jacs.0c04619
J. Am. Chem. Soc. 2020, 142, 17346−17355